RSC Sustainability

ROYAL SOCIETY OF CHEMISTRY

PAPER

View Article Online
View Journal | View Issue

Cite this: *RSC Sustainability*, 2023, **1**, 357

The adsorption kinetics and mechanism of odorous gases onto textile fibers†

Wenli Bai,[a] Hao Yu,[b] Longlong Liu,[c] Esfandiar Pakdel,[a] Bin Tang,[a] Hongli Su,[a] Christopher Hurren,[a] Lei Liu,[c] Jinfeng Wang*[b] and Xungai Wang*[de]

Malodor is regarded as a very significant nuisance, 2nd only to noise pollution, in the developed world. It directly impacts people's health and wellbeing. The prevention of odor build-up is a key property for both interior textiles and active sportswear. Traditional approaches for odor elimination rely on textile surface treatment. However, the role of intrinsic morphology and chemical composition of fibers in odor elimination has not been taken into account. In this study, the adsorption characteristics and mechanisms of three common types of fibers (wool, cotton and nylon) for two typical odors of acetic acid and ammonia were systematically investigated through kinetic modelling, the inverse gas chromatography (IGC) technique, and density functional theory (DFT) calculations. Both acetic acid and ammonia adsorption onto fibers followed a pseudo-second-order kinetic model. Among all the tested fibers, wool showed the highest adsorption ability towards both acetic acid and ammonia. The adsorption behaviors of cotton and nylon were explored based on quantitative measurement of surface Lewis acid-base properties using the IGC technique. These findings were further corroborated by DFT calculations *via* the interactions between fibers and the adsorbed odor. This study provides a new insight into odor adsorption onto commonly used fibers and their interactions, which is a key step in developing fibrous materials for odor control, including body odor and indoor air pollutants.

Received 31st October 2022
Accepted 19th January 2023

DOI: 10.1039/d2su00086e

rsc.li/rscsus

Sustainability spotlight

Odor is a topic relevant to people's health and wellbeing, and malodor is also regarded as the 2nd most significant nuisance in the developed world (after noise pollution). Children, older people, and other vulnerable persons are especially sensitive to low levels of air pollution. Increasing concerns about indoor air quality in recent years have urged research on the odor adsorption quality of textile products. Clarifying the adsorption mechanism of odor on textile fibers can improve the indoor air quality using textile odor control technologies. This work aligns with the UN SDG of ensuring healthy lives and promoting well-being for all at all ages.

1. Introduction

Ammonia and carboxylic acids like acetic acid play an important role in the generation of odor pollution in indoor air.[1] One of their sources is emission from humans and pets through skin, urine and feces. Other indoor sources include cooking, smoking and cleaning products.[1,2] These two airborne odors have the potential to cause olfactory nerve-mediated smell sensations and trigeminal nerve-mediated irritation sensation, typically burning, tingling, or prickling.[3,4] Exposure to these two common odors is also associated with the prevalence of several symptoms, such as headache, nausea, and eye and throat irritation.[4]

The fibrous materials used in interior textiles are mainly synthetic fibers (*e.g.*, nylon and polyester) and natural fibers (*e.g.*, wool and cotton). Textile products such as curtains and carpets have a great influence on indoor air quality because they can act as air filters and provide substantial surface area for airborne pollutant adsorption *via* a sink effect mechanism.[5–7] The chemical structure and physical properties of fibers play a significant role in determining gaseous pollutant adsorption/desorption characteristics onto fibrous materials. A number of fibrous materials have been investigated in terms of their odor retention and emission performance by considering fiber types,

[a]*Institute for Frontier Materials, Deakin University, Geelong/Melbourne, Victoria 3216, Australia*

[b]*National Local Joint Laboratory for Advanced Textile Processing and Clean Production, Wuhan Textile University, Wuhan 430073, China*

[c]*Center for Computational Chemistry, College of Chemistry and Chemical Engineering, Wuhan Textile University, Wuhan 430073, China*

[d]*JC STEM Lab of Sustainable Fibers and Textile, School of Fashion and Textiles, The Hong Kong Polytechnic University, Hung Hom, Kowloon, Hong Kong*

[e]*Research Institute for Sports Science and Technology, The Hong Kong Polytechnic University, Hung Hom, Kowloon, Hong Kong. E-mail: xungai.wang@polyu.edu.hk*

† Electronic supplementary information (ESI) available: Odor detection system; correlation coefficients (R^2) from kinetic models; surface property parameters; wool fiber diameter effect on acetic acid adsorption performance. See DOI: https://doi.org/10.1039/d2su00086e

odor detection methods, and fabric structures.[8–11] For example, the adsorption/desorption performances of α-pinene and toluene onto/from wool carpet, nylon carpet, cotton curtain materials were measured using a chamber testing method.[12] It was found that all three interior textile materials showed higher adsorption for α-pinene than for toluene. The adsorption capacities for both VOCs followed the order of wool carpet > nylon carpet > cotton curtain. The kinetics and thermodynamics of ammonia adsorption onto wool and cotton fibers were investigated by dynamic monitoring experiments using time-resolved infrared spectroscopy.[13] The Langmuir isotherm model well describes ammonia adsorption onto both wool and cotton fibers.

Meanwhile, wool can be utilised as an odor adsorbent to control body odor.[13] Body odor emanation from textiles may be partially caused by the metabolism of bacteria, but the chemical composition and physical morphology of fiber also play an important role in determining the textiles' ability to retain body odor.[14] For instance, under low concentrations of odor, a wool/polyester blend containing 20% wool showed substantially higher adsorption ability towards ammonia, acetic acid and butyric acid than 100% polyester fabric.[15] Both physical and chemical interactions are involved in odor molecule adsorption onto fibrous materials.[16,17]

Absorption of foul-smelling substances by different textile fabrics was reported and it was found that the amount of absorption was largely dependent on the type of fibers.[18] In addition, the amount of sorption increased nearly in proportion to the moisture content of fibers. However, how the fiber types with different physical structures and chemical compositions affect their adsorption capacities and odor selective adsorption properties has not been quantitatively revealed yet. In this study, the real-time monitoring of the adsorption/desorption process of acetic acid and ammonia onto wool, cotton and nylon was investigated by infrared-based spectroscopic technology. Acetic acid and ammonia were used as the representatives of common acidic and basic model gases, respectively, which exist in indoor living spaces, body sweat, and excrement odors. Kinetic studies involved in the adsorption of odor onto fibers were conducted to give a comprehensive understanding of the deodorizing process of textiles. The inverse gas chromatography (IGC) technique and density functional theory (DFT) calculations were employed to quantitatively investigate the interaction between the fiber surface and odor molecules. The findings of this study can clarify the odor adsorption behavior of the three commonly used types of fibers, promoting the application of these fibers in a broad range of applications such as medical textiles, anti-odor apparel, fragrant fabrics, and odor-absorbing textiles.

2. Experimental section

2.1 Materials

Three fiber types including wool, cotton and nylon were tested. Raw wool samples from merino sheep were supplied by a farm in New South Wales, Australia and were scoured before use.[19] Clean cotton and nylon (polyamide 6,6) samples were sourced from Australian mills and used as received without further treatment. All clean samples were conditioned in a standard conditioned laboratory (temperature: 20 ± 2 °C, humidity: 65 ± 2%) for 24 hours before testing. The specifications for these fiber samples are listed in Table 1. Ammonium hydroxide (28–30 wt% solution of NH_3 in water; $\rho = 0.9$ g mL^{-1}) and acetic acid (glacial, ≥99.7%) were purchased from Sigma-Aldrich.

Table 1 The specifications of wool, cotton and nylon fibers[a]

Sample	Diameter (μm)	CV_D (%)
Wool	16.5	16.4
Cotton	14.7[b]	19.0
Nylon	17.9	10.5

[a] CV_D: Coefficient of variation for diameter. [b] Ribbon width.

2.2 Characterization

Fiber diameters of clean wool and nylon loose samples were determined using an optical fiber diameter analyzer (OFDA) 2000 (BSC Electronics, Australia) according to the ASTM D6500 standard. The fineness (ribbon width) of cotton fiber samples was obtained using a Cottonscope instrument (BSC Electronics, Australia) based on the ASTM standard. A Supra 55VP scanning electron microscope (SEM, Carl Zeiss AG, Germany) was used to observe the surface morphology of wool, cotton and nylon fibers with Au coating (Lecia EM ACE600, Australia). Chemical compositions of the fibers were studied by Fourier-transform infrared spectroscopy (FTIR, Bruker Vertex 70, Germany) using the ATR method with a scan resolution of 4 cm^{-1} and 64 scans per sample in a range of 600 to 4000 cm^{-1}.

Surface heterogeneous properties of wool, cotton and nylon fibers were characterized using a commercial inverse gas chromatography-surface energy analyzer (IGC-SEA, Surface Measurement Systems, UK). Methane was used as a reference probe for dead volume correction. The Brunauer–Emmett–Teller (BET) specific surface areas of the three fiber types were measured using octane as a non-polar probe. Two runs were conducted for each sample and the average value was calculated under conditions where the BET equation showed good linearity ($R^2 \geq 0.995$). Three non-polar *n*-alkane probes (heptane, octane and nonane) were used to measure the dispersive surface energy profiles of the fiber samples within a determined surface coverage range (n/n_m = 0.01–0.3). Five polar probes (dichloromethane, chloroform, ethyl acetate, ethanol and acetone) were chosen to measure the specific surface energy and acid-base parameter profiles. All samples were measured under the same conditions (30 °C, 0% RH) using helium as the carrier gas at a flow rate of 10 mL min^{-1}. Prior to measurement, all the samples were pre-conditioned at testing temperature (30 °C) for 1 h. SEA analysis software was used to analyze the obtained data. Peak Com, Della Volpe scale, Schultz method and BET theory were applied for this analysis.[20–23]

2.3 Dynamic odor adsorption and emission monitoring

Dynamic monitoring of acetic acid and ammonia adsorption on the three fiber types was carried out in an air-tight odor detection system that included a gas circulating pump, sample

chamber, infrared-based gas analyzer and data collector (Fig. S1†). The quantitative analysis of the odor concentration in the detection system was achieved by measuring the time-resolved infrared absorption intensities of acetic acid and ammonia at a wavelength of 8.5 μm and 10.4 μm, respectively.[15] All dynamic adsorption and emission experiments were carried out at room temperature in a fume hood. To investigate the effect of fiber types on odor adsorption behavior, samples from different fiber types (2.0 g) were placed in the sample chamber, and then a determined volume of acetic acid (4.3 μL) or ammonia solution (5 μL) was injected into the gas pump using a micro-syringe, which was quickly gasified and circulated in the odor detection system. The amount of acetic acid and ammonia used for this test was maintained at the same parts per million volume (ppmv) for all the fiber samples.

To monitor the corresponding odor emission process, a fiber sample (2.0 g) was placed in a sealed container together with a determined volume of acetic acid or ammonia (10 μL), which was then kept for 12 h at room temperature to reach its odor adsorption equilibrium. The fiber samples were then placed in the sample chamber and sealed. Odor emission intensity (absorbance reading) was directly recorded using an IR-based spectrometer.

The quantity of adsorbed acetic acid or ammonia on each fiber sample (q_t) at time (t) was determined using eqn (1):[24]

$$q_t = \frac{(C_0 - C_t)V}{M} \quad (1)$$

where C_0 represents the initial odor concentration (mg L^{-1}), C_t represents the concentration of odor (mg L^{-1}) at any time t (min), V is 8 L for the volume of the detection system and M (g) is the mass of the fiber sample. The equilibrium adsorption quantity (q_e) is obtained when adsorption reaches equilibrium under testing conditions.

2.4 Kinetic adsorption models

Adsorption kinetic studies may not only predict adsorption experimental results but also provide important parameters such as adsorption rate constants for evaluating the adsorption process and efficiency.[25] Generally, three consecutive steps were involved throughout the adsorption process, which include external mass transfer, intra-particle diffusion, and adsorption reaction.[26,27] Two intra-particle diffusion models (Dunwald–Wagner model and the Weber–Morris model) were adopted to describe the diffusion stage in the adsorption process. Two adsorption reaction kinetic models including the pseudo-first-order model and pseudo-second-order model were applied to fit the adsorption reaction process.

2.4.1 Dunwald–Wagner (D–W) model. The D–W model is presented using the following equations:[28]

$$\log(1 - F^2) = -\frac{k}{2.303}t \quad (2)$$

$$F = \frac{q_t}{q_e} \quad (3)$$

where k is the diffusion rate constant (min^{-1}), which can be obtained by plotting $\log(1-F^2)$ against t. q_t (mg g^{-1}) and q_e (mg g^{-1}) are the odor adsorption quantity of the fiber adsorbent at contact time and at equilibrium, respectively. F is the odor removal percent calculated using q_t/q_e.

2.4.2 Weber–Morris (W–M) model. The W–M model, as one of the intra-particle diffusion models, is commonly applied to describe the intraparticle diffusion process.[29]

The W–M model is expressed as follows:

$$q_t = k_{id}t^{1/2} + C \quad (4)$$

where k_{id} (mg g^{-1} $min^{-1/2}$) is the intra-particle diffusion rate constant and C is the boundary layer thickness. q_t (mg g^{-1}) is the odor adsorption quantity of the fiber adsorbent at time t. The rate constant k_{id} and C can be obtained by plotting q_t against $t^{1/2}$. Intraparticle diffusion would be the rate controlling step if the plot of q_t *vs.* $t^{1/2}$ is a straight line and goes through the origin (0, 0).

2.4.3 Pseudo-first-order (PFO) model. The PFO model could represent three conditions, which include (i) when the initial concentration of the adsorbate (target molecules capable of being adsorbed) (C_0) is high,[30] (ii) when the adsorption process is in its initial stage,[31] and (iii) when the adsorbent material has a few active sites or few adsorptive sites that can interact with the active sites.[29,32]

The differential form of the PFO model is given as:[33]

$$\text{PFO rate} = \frac{dq_t}{dt} = k_1(q_e - q_t) \quad (5)$$

The linearized PFO model is expressed as:

$$\ln(q_e - q_t) = \ln q_e - k_1 t \quad (6)$$

where q_t (mg g^{-1}) is the odor adsorption quantity of the fiber adsorbent at contact time t and q_e (mg g^{-1}) is the equilibrium adsorption quantity obtained using the PFO model. k_1 is the PFO rate constant (min^{-1}). The rate constant (k_1) and adsorption quantity at equilibrium were calculated from the slope and intercept of the plot of ln ($q_e - q_t$) against t.

2.4.4 Pseudo-second-order (PSO) model. The PSO model could represent three conditions, which include (i) when the value of C_0 is low, (ii) the final stage of the adsorption process and (iii) when the adsorbent is abundant with active sites.[29]

It has been proposed that the adsorption rate of PSO is related to the adsorbent's surface vacant adsorption sites rather than the adsorptive concentration in bulk.[34]

$$\text{PSO rate} = \frac{dq_t}{dt} = k_2(q_e - q_t)^2 \quad (7)$$

The linearized PSO model is presented as:

$$\frac{t}{q_t} = \frac{1}{k_2 q_e^2} + \frac{t}{q_e} \quad (8)$$

The initial adsorption rate h_2 (mg g^{-1} min^{-1}) is expressed as

$$h_2 = k_2 q_e^2 \quad (9)$$

where q_t (mg g^{-1}) is the odor adsorption quantity of the fiber adsorbent at contact time t and q_e (mg g^{-1}) is the equilibrium adsorption quantity calculated using the PSO model. k_2 is the PSO rate constant (g mg^{-1} min^{-1}), which is used to describe the rate of adsorption equilibrium. The equilibrium adsorption quantity (q_e) and the rate constant (k_2) can be calculated from the slope and intercept of the plot of t/q_t *versus* t.[35]

The linear form of these models was applied to correlate the experimental results of the acetic acid and ammonia adsorption onto fibrous adsorbents. The coefficient of determination (R^2) was used to identify the best fitting adsorption model among the above models, and related parameters were calculated and presented.

2.5 Density functional theory calculations

All density functional theory (DFT) calculations were performed by employing the Gaussian 09 package.[36] The structures were optimized at the Grimme'D3(BJ)[37] corrected B3LYP level of theory[38] in conjunction with the 6-311+G* basis set.[39,40]

The adsorption energy of odor molecules on a fiber surface was calculated using the following equation:

$$E_{ads} = E_{fiber+odor} - (E_{fiber} + E_{odor}) \quad (10)$$

where $E_{(fibre+odor)}$, E_{fiber} and E_{odor} represent the energies of the adsorption system, fiber and free odor molecules, respectively. A negative value of the adsorption energy indicates a favorable adsorption process.

3. Results and discussion

3.1 Adsorption and emission performance

Three different fiber types, including wool, cotton and nylon, were used for odor adsorption tests (Fig. 1a–c). The typical morphology structures of the three fiber types showed that wool fiber had overlapping scales on the surface (Fig. 1d). Cotton fibers had a twisted ribbon-like structure with an uneven fiber surface including wrinkles and grooves (Fig. 1e). Nylon which is a synthetic fiber had a smooth and uniform surface (Fig. 1f).

Acetic acid and ammonia were used as model molecules to evaluate the odor adsorption performance of fiber samples. The typical odor adsorption and desorption performance of the three different fiber types is shown in Fig. 2. All three different fiber types can greatly adsorb acetic acid in its gaseous form (Fig. 2a). Without a fiber adsorbent, the acetic acid concentration slowly decreased and reached equilibrium, which may be caused by the odor condensation on the inner wall of the testing chamber. In the presence of wool fiber, this concentration was reduced to almost 0 after 120 min of adsorption. This is compared with 0.15 mg L^{-1} acetic acid left in the system for nylon fiber and 0.2 mg L^{-1} for cotton fiber. Therefore, the acetic acid adsorption performance for the three fiber samples followed the order of wool > nylon > cotton. The desorption performance of acetic acid from these fiber samples was also investigated (Fig. 2b). Wool fiber showed negligible emission of acetic acid even after 120 minutes of desorption time. Cotton showed the highest acetic acid desorption among the three samples.

Fig. 2c shows the adsorption performance of ammonia on the three fiber types. Wool fiber demonstrated the highest ammonia adsorption amount among the three samples, followed by cotton fiber. Nylon fiber showed the least adsorption amount of ammonia among the three fiber samples. Ammonia emission processes of the three fiber samples were also studied, and wool showed the lowest emission with almost no ammonia detected (Fig. 2d). This is compared with cotton showing a quick increase in ammonia emission intensity during the

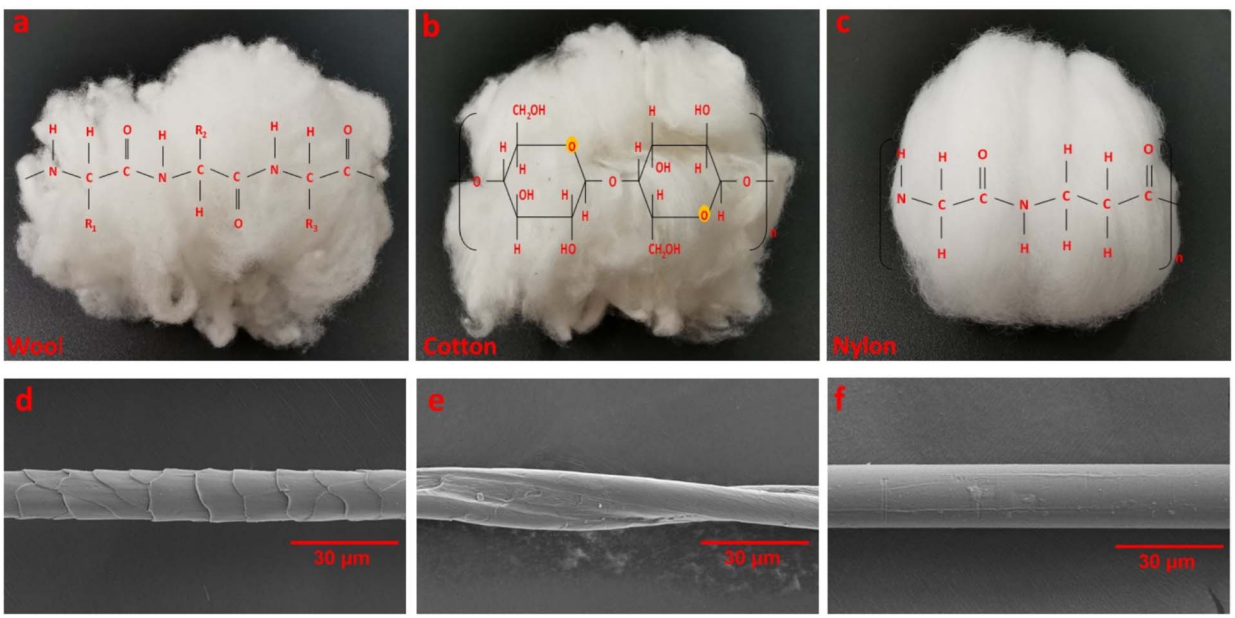

Fig. 1 The photographs and SEM images of fiber samples for odor adsorption: wool (a and d), cotton (b and e) and nylon (c and f).

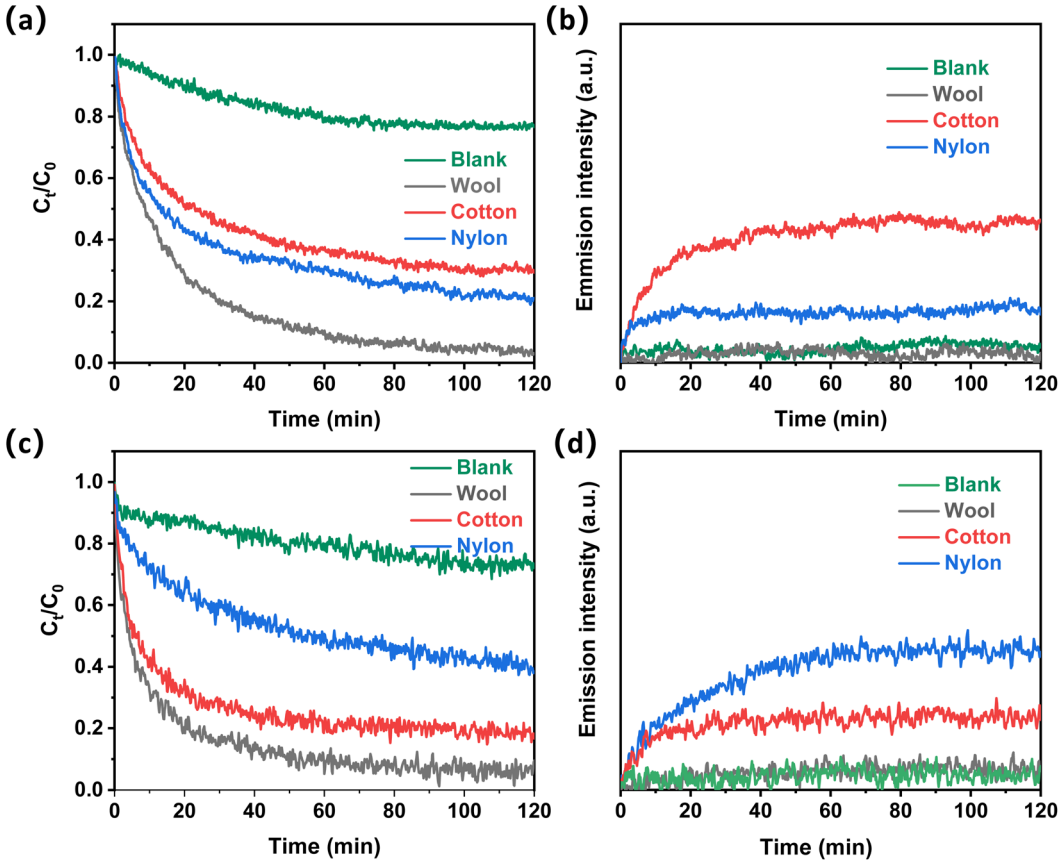

Fig. 2 Acetic acid (a) and ammonia (c) concentration change in the odor detection system in the presence of the same weight of wool, cotton, and nylon fibers (2.0 g); the time-dependent variation of acetic acid (b) and ammonia (d) emission intensity for wool, cotton and nylon fiber samples.

initial 10 min and nylon showing the highest emission intensity among the three samples under the same test conditions.

3.2 Adsorption kinetic study

Adsorption kinetics describes the uptake rates of acetic acid and ammonia onto fiber samples, which will promote understanding of the adsorption process and predict equilibrium adsorption quantity for odor control applications. Because mass transfer is a very fast process in this work, the atmosphere was circulated *via* a gas pump and mass transfer is not considered in the kinetic process. Two diffusion models (Dumwald–Wagner model and the Weber–Morris model) and two adsorption reaction models (pseudo-first-order model and the pseudo-second-order model) were used to analyze the experimental data for acetic acid and ammonia adsorption onto the three different fiber types.

The adsorption quantity (q_t) of acetic acid onto wool, cotton, and nylon with contact time (t) is shown in Fig. 3a. It can be observed that wool fiber demonstrated the highest adsorption quantity towards acetic acid, which was followed by nylon and cotton fiber. The equilibrium adsorption capacity of acetic acid was measured to be 2.54 mg g^{-1}, 2.11 mg g^{-1} and 1.87 mg g^{-1} for wool, nylon, and cotton, respectively. Fig. 3b–e show the kinetic model plots for acetic acid removal with the three fiber types under the same conditions. According to the correlation coefficient R^2 of the four kinetic models in different time ranges (Tables S1 and S2†), it was found that the acetic acid adsorption onto the three fiber types fits different models. Within the initial 10 min, the adsorption process fits better for diffusion models (D–W model and the W–M model) than for reaction models (PFO model and the PSO model), which indicated that the initial adsorption of acetic acid onto wool, cotton, and nylon fiber was mainly controlled by the intraparticle diffusion process.[30]

As the adsorption time increased from 10 min to 120 min, the correlation coefficient R^2 of both the D–W model and the W–M model decreased, while the value of R^2 from the PSO model was higher than 0.99 (Fig. 3e), indicating that the overall adsorption process of acetic acid onto the three fiber types followed the PSO model. The equilibrium adsorption capacity ($q_{e,cal}$) calculated from the PSO model was also found to be close to the experimental ($q_{e,exp}$) values (Table 2). It was reported that the adsorption of the PSO model was related to the surface vacant adsorption sites.[34] Initial adsorption rates (h_2) of acetic acid onto the three fiber types based on the PSO model were calculated (Table 2), which follow the order of wool (0.308) > nylon (0.212) > cotton (0.177). This result indicates that wool fiber contains the most active sites for acetic acid affinity, followed by nylon and cotton.

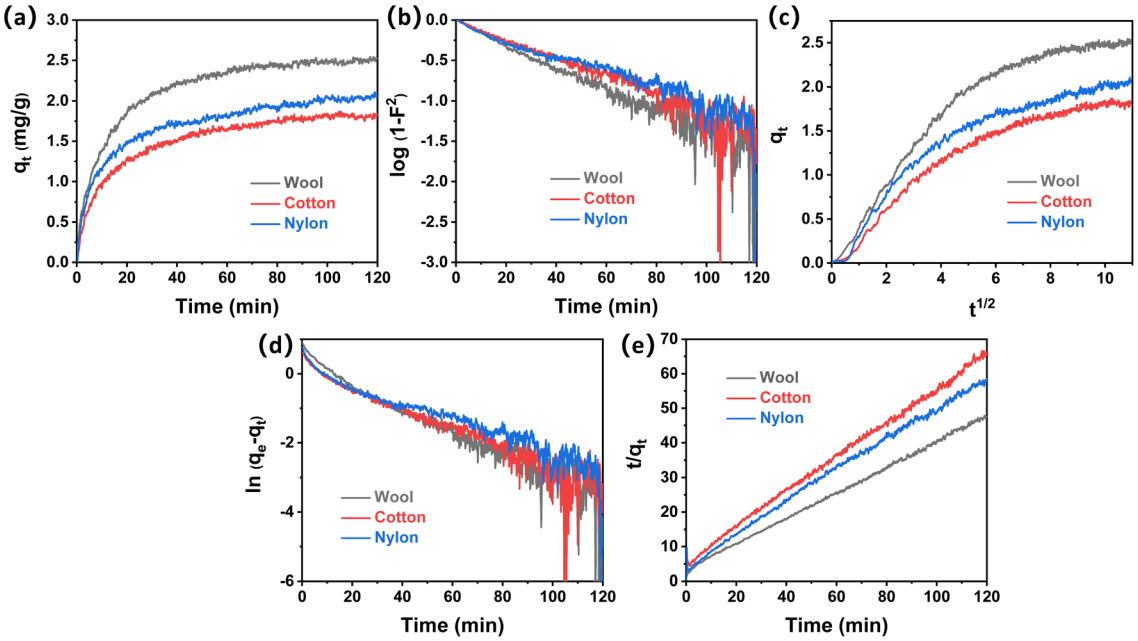

Fig. 3 Time effect on the adsorption quantity of acetic acid onto wool, cotton, and nylon (2.0 g) at room temperature (a); adsorption diffusion kinetic models of acetic acid onto wool, cotton and nylon fibers: D–W model (b) and W–M model (c); adsorption reaction kinetic models of acetic acid onto wool, cotton and nylon fibers: PFO model (d) and PSO model (e).

Table 2 Adsorption kinetic model parameters for acetic acid adsorption onto wool, cotton, and nylon fibers

	Parameters	Wool	Cotton	Nylon
Kinetic models	$q_{e,exp}$ (mg g^{-1})	2.543	1.868	2.108
D–W model	k (min^{-1})	1.31×10^{-2}	1.19×10^{-2}	9.94×10^{-3}
	R^2	0.9019	0.9062	0.9131
W–M model	k_{id} (mg g^{-1} min$^{-1/2}$)	0.162	0.127	0.129
	C	0.981	0.602	0.779
	R^2	0.8251	0.8802	0.8721
PFO model	$q_{e,cal}$ (mg g^{-1})	1.419	1.235	1.211
	k_1 (min^{-1})	3.28×10^{-2}	3.04×10^{-2}	2.55×10^{-2}
	R^2	0.9134	0.9249	0.9296
PSO model	$q_{e,cal}$ (mg g^{-1})	2.696	1.998	2.198
	k_2 (g mg^{-1} min^{-1})	4.24×10^{-2}	4.43×10^{-2}	4.39×10^{-2}
	h_2 (mg g^{-1} min^{-1})	0.308	0.177	0.212
	R^2	0.9993	0.9985	0.9974

The adsorption quantity (q_t) of ammonia onto wool, cotton, and nylon fibers with contact time (t) is shown in Fig. 4a. It can be observed that wool fiber demonstrated the fastest adsorption rate towards ammonia, which was followed by cotton and nylon fiber.

The equilibrium adsorption quantities of wool, cotton and nylon for ammonia were measured to be 0.49 mg g^{-1}, 0.42 mg g^{-1}, and 0.32 mg g^{-1}, respectively. Fig. 4b–e show four kinetic model plots for ammonia removal in the presence of the three fiber types. All the correlation coefficients R^2 (Tables S3 and S4†) from the four adsorption kinetic models were less than 0.99 within the initial 10 min, indicating that neither the diffusion step nor the adsorption step was the only rate-limiting step at the beginning of ammonia adsorption onto these fiber samples. This means that both steps proceeded very quickly in the case of ammonia adsorption onto the three fiber samples at the beginning of 10 min; this may be because of the smaller molecular size of ammonia compared to acetic acid.

Fig. 4e shows that t/q_t has a good linear relationship with a high R^2 value of over 0.99, suggesting that the overall adsorption reaction process of ammonia onto the tested fibers followed the PSO model. The calculated equilibrium adsorption capacity ($q_{e,cal}$) from the PSO model was close to the practical experimental values ($q_{e,exp}$). Initial adsorption rates (h_2) of ammonia onto the three fiber types based on the PSO model were determined (Table 3). The initial adsorption rate (h_2) of

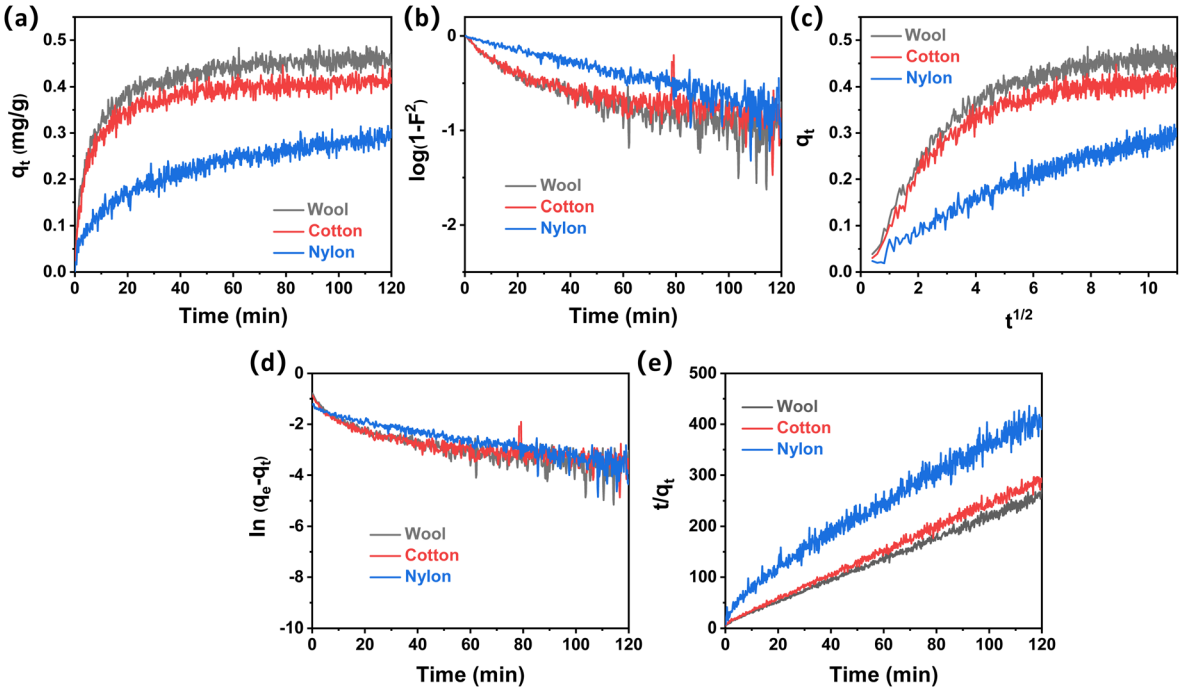

Fig. 4 The effect of time on the adsorption quantity of ammonia onto wool, cotton and nylon fibers (2.0 g) at room temperature (a); adsorption diffusion kinetic models of ammonia onto wool, cotton and nylon fibers: D–W model (b) and W–M model (c); adsorption reaction kinetic models of ammonia onto wool, cotton and nylon fibers: PFO model (d) and PSO model (e).

Table 3 Adsorption kinetic model parameters for ammonia adsorption onto wool, cotton and nylon fibers

	Parameters	Wool	Cotton	Nylon
Kinetic models	$q_{e.exp}$ (mg g^{-1})	0.491	0.417	0.318
D–W model	k (min^{-1})	7.38×10^{-3}	5.85×10^{-3}	7.14×10^{-3}
	R^2	0.6405	0.5638	0.7144
W–M model	k_{id} (mg g^{-1} $min^{-1/2}$)	2.25×10^{-2}	1.96×10^{-2}	2.22×10^{-2}
	C	0.253	0.231	6.50×10^{-2}
	R^2	0.7101	0.6802	0.9241
PFO model	$q_{e.cal}$ (mg g^{-1})	0.228	0.142	0.163
	k_1 (min^{-1})	1.94×10^{-2}	1.51×10^{-2}	1.86×10^{-2}
	R^2	0.6213	0.4434	0.5301
PSO model	$q_{e.cal}$ (mg g^{-1})	0.480	0.428	0.326
	k_2 (g mg^{-1} min^{-1})	0.428	0.507	0.174
	h_2 (mg g^{-1} min^{-1})	0.0986	0.0929	0.0185
	R^2	0.9966	0.9964	0.9808

wool (0.0986) was slightly higher than that of cotton, which was over 5 times higher than that of nylon (0.0185). This result indicated that wool fiber possessed the most active sites for ammonia adsorption among the other tested fibers, while nylon showed a lack of active sites for ammonia affinity.

3.3 Insight into the adsorption mechanism

To gain an insight into the influence of the intrinsic fiber composition on the odor adsorption properties of fiber samples, inverse gas chromatography (IGC) was used to quantitatively measure the surface property parameters of the three fiber types. The dispersive (van der Waals) and specific (Lewis acid-base) surface energy profiles of wool, cotton and nylon fibers at varied surface coverage are displayed in Fig. 5a. At 0.1 surface coverage, the dispersive surface energy (γ_s^D) for the three fiber types followed the order of wool (49.1 mJ m^{-2}) > cotton (40.8 mJ m^{-2}) > nylon (37.1 mJ m^{-2}), indicating that wool fiber showed the highest odor adsorption potential *via* physical interaction, which was followed by cotton and nylon, whereas the specific surface energy (γ_s^{sp}) for the three fiber types followed the order of nylon (9.6 mJ m^{-2}) > wool (7.9 mJ m^{-2}) > cotton (5.9 mJ m^{-2}), suggesting that nylon fiber demonstrated the best adsorption potential *via* chemical interaction.[41] The dispersive surface energy was higher than the specific surface energy for all

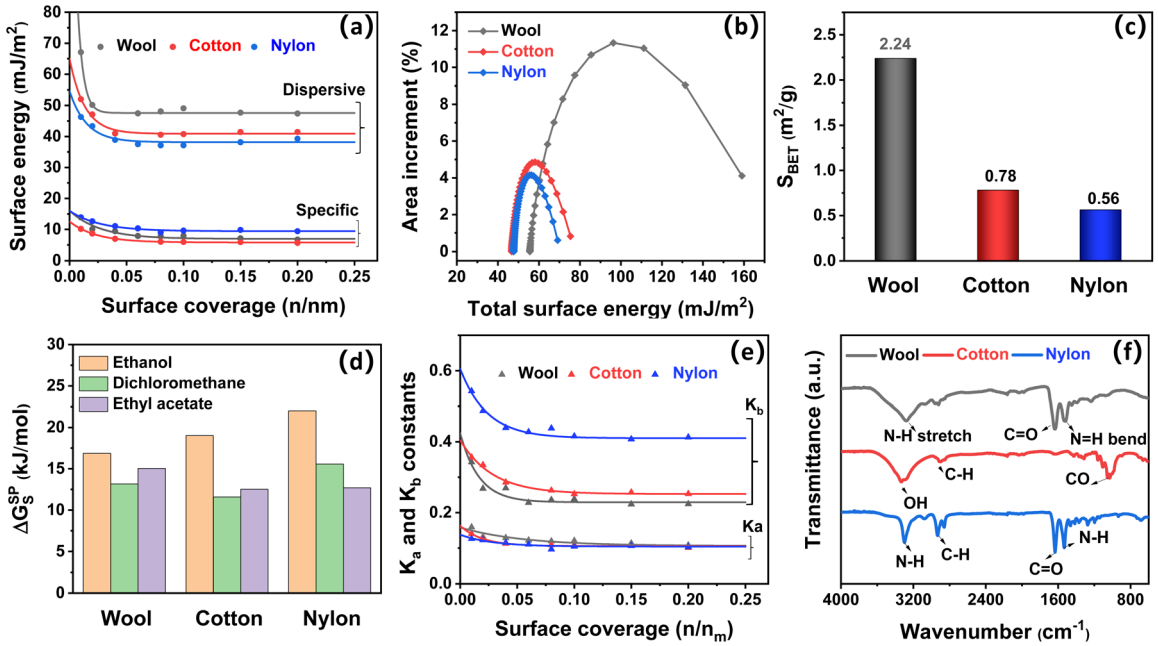

Fig. 5 Dispersive and specific surface energy profiles (a); distribution profiles of total surface energy (b); specific surface area (c); specific free energy of adsorption of polar probes at 0.1 surface coverage (d); Gutmann acid-base constants (Ka and Kb) profiles (e); FTIR spectra (f) of wool, cotton and nylon fibers.

three fiber types, revealing that the potential for physisorption was higher than that of the chemisorption for all three fibers. Total surface energy (γ_s^T) is the combination of dispersive and specific surface energies, which represents the number of active sites per unit surface.[41] Meanwhile, wool showed a broad distribution profile of total surface energy (Fig. 5b), which indicated that it had a large surface heterogeneity due to its complex physical structure (overlapping cuticles) and chemical composition (eighteen kinds of proteins).[42] Compared to wool, cotton fiber and synthetic nylon fiber showed a narrow distribution profile of total surface energy, which indicated their unitary composition and homogeneous surface morphology as confirmed by the SEM results. The surface morphology difference also correlated with the specific surface area (S_{BET}) order of the three fiber types, which was wool (2.24 $m^2\ g^{-1}$) > cotton (0.78 $m^2\ g^{-1}$) > nylon (0.56 $m^2\ g^{-1}$) (Fig. 5c).[22]

Given that high surface energy and large specific surface area can provide significant adsorption sites for gas affinity and thus improve the adsorption performance of the fibers materials *via* physisorption or chemisorption,[43] wool fiber has both the highest surface energy and the largest surface area among the three fiber types, so it showed the best adsorption performance for both acetic acid and ammonia (Fig. 2). Similarly, cotton demonstrated better adsorption ability towards ammonia than nylon due to its higher concentration of adsorption sites. However, this is not the case for acetic acid adsorption onto cotton and nylon. Nylon showed remarkable uptake towards acetic acid with an adsorption quantity of 2.11 mg g^{-1}, while the amount was 1.87 mg g^{-1} for cotton fiber (Fig. 3a). As nylon has the lowest specific surface area, chemical interaction might be the main mechanism for acetic acid adsorption onto nylon.

To figure out the role of chemical (Lewis acid-base) interaction in the adsorption behavior of wool, cotton and nylon fiber, the surface acid-base nature of the three fiber types was evaluated based on their interactions with different polar probes, including dichloromethane, ethyl acetate, acetone, chloroform and ethanol (Fig. S2†).[41] Higher specific free energy (ΔG_s^{sp}) indicates a stronger Lewis acid-base interaction between polar probes and the fiber surface. As shown in Fig. 5d, the adsorption specific free energy of the three fibers on amphoteric molecules (ethanol) was the highest, indicating that the surfaces of all three fibers are amphoteric with both acidic (electron acceptor) and basic (electron donor) adsorption sites (Fig. 5e).[23] The specific adsorption free energies of the basic probe (ethyl acetate) and acidic probe (dichloromethane) onto wool fiber were higher than those onto cotton, indicating that there is stronger Lewis acid-base interaction between odor molecules and wool fiber. This result agrees with the excellent odor retention ability of wool with negligible odor emission (Fig. 2b and d). As expected, the specific free energy value of nylon was the highest with acidic probes (dichloromethane) among the three fiber types, which was consistent with the adsorption behavior of acetic acid onto nylon fiber. Lewis acid-base constant (K_a and K_b) profiles were also determined and are shown in Fig. 5e and summarized in Table. S5.† The surface basicity (K_b/K_a) of nylon was measured to be 3.98, indicating the predominant basic nature of nylon fiber and hence facilitating the adsorption of acidic odor (acetic acid).

Surface functional groups are important adsorption sites for gaseous acetic acid and ammonia affinity, which were identified by FTIR as shown in Fig. 5f. Wool is composed of proteins with many functional groups, including amide (peptide) bonds,

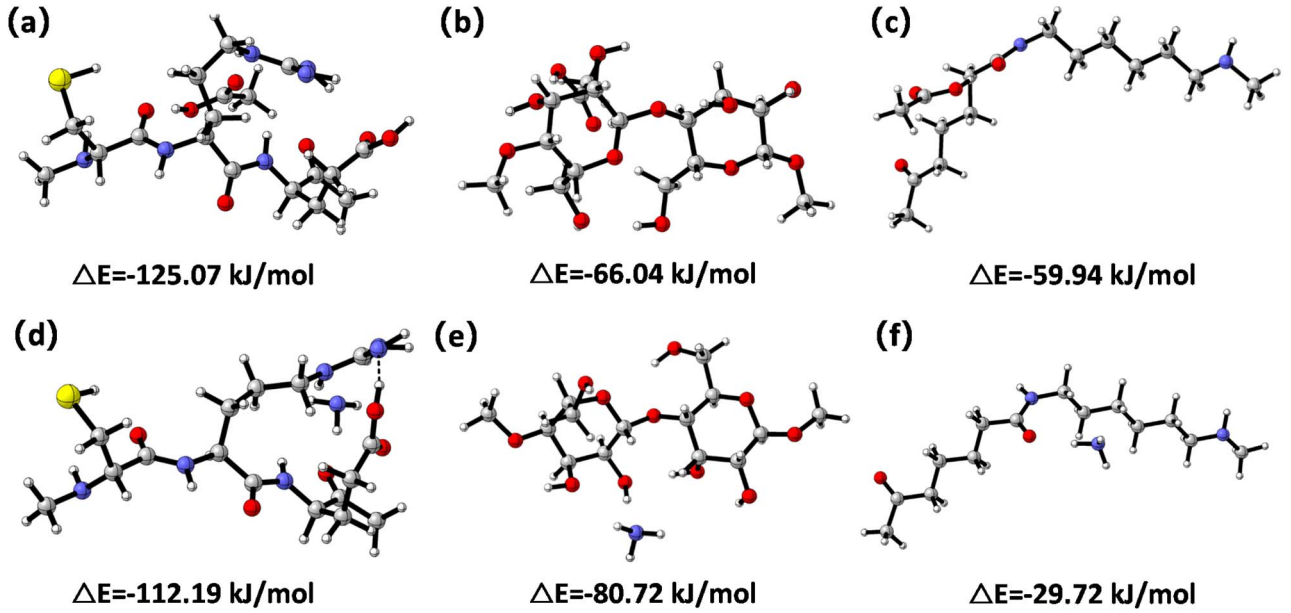

Fig. 6 The most stable acetic acid adsorption configuration on wool (a), cotton (b) and nylon fiber (c); and the most stable ammonia adsorption configuration onto wool (d), cotton (e) and nylon fiber (f).

cystine (disulphide) crosslinks, and side chains of amino acid residues. The bands at around 3280 cm^{-1}, 1641 cm^{-1} and 1519 cm^{-1} (Amide II) of wool fiber were associated with the N–H bond stretching (Amide A), C=O (Amide I) stretching vibration, and N–H (Amide II) bending vibration, respectively, which can provide adsorption sites for both acetic acid and ammonia odor molecules.[24,44] Hydroxyl groups (–OH) observed at around 3334 cm^{-1} are active acidic sites (electron acceptors) that benefit the interaction between cotton and ammonia.[13] Nylon was predominantly basic in nature due to its amide groups (–C(O)NH–), which appeared as two strong peaks at 1634 cm^{-1} and 1538 cm^{-1}, corresponding to amide I (C=O) and amide II (N–H) bands, respectively. These basic adsorption sites contributed to a strong interaction between nylon and acetic acid molecules.

To further clarify the interaction between the three fiber types and odor molecules, the adsorption energies of acetic acid and ammonia onto fiber samples were obtained *via* DFT calculations (Fig. 6). The adsorption energy of physical adsorption was about 40 kJ mol^{-1}, and the adsorption energy of the chemical adsorption process was equivalent to the heat of the chemical reaction, which is generally 84–417 kJ mol^{-1}.[45] Adsorption energies of acetic acid and ammonia attached on the wool fiber were calculated to be −125.07 kJ mol^{-1} (Fig. 6a) and −112.19 kJ mol^{-1} (Fig. 6d), respectively. This result indicated that chemical adsorption occurred during the odor adsorption processes onto wool, which may have included acetic acid interacting with a basic amino acid (*e.g.* arginine) and ammonia interacting with an acidic amino acid (*e.g.* glutamic acid).[24,46] Acetic acid and ammonia adsorbed on the cotton fiber surface led to adsorption energies of −66.04 kJ mol^{-1} (Fig. 6b) and −80.72 kJ mol^{-1} (Fig. 6e), respectively. These values indicated that cotton fiber had a stronger adsorption towards ammonia than acetic acid. This could be because acetic acid was unable to react with cellulose to form stable acetyl groups,[47] whereas hydroxyl groups (–OH) on the cotton fiber surface acted as active acidic sites (electron acceptors) to benefit the interaction between cotton and ammonia *via* hydrogen bonding.[13] The adsorption energies of acetic acid and ammonia adsorbed on the nylon fiber surface were −59.94 kJ mol^{-1} (Fig. 6c) and −29.72 kJ mol^{-1} (Fig. 6f), respectively, suggesting that nylon fiber was more likely to attract acetic acid than ammonia. This may be attributed to the formation of a hydrogen bond between the amino groups of nylon and acetic acid.[48] As a result of the reversible process of physical adsorption and weak Lewis acid-base interaction between fiber adsorbents and odors, their adsorption ability can be recovered by placing the textile samples in a conditional lab with an air flow for 12 hours.[41]

4. Conclusions

In summary, this work systematically investigated the adsorption characteristics and mechanisms of three common textile fibers, wool, cotton, and nylon, for two typical odors of acetic acid and ammonia. The acetic acid adsorption quantities of the three fiber types followed the order of wool (2.54 mg g^{-1}) > nylon (2.11 mg g^{-1}) > cotton (1.87 mg g^{-1}), while ammonia adsorption quantities of the three fiber types followed the order of wool (0.49 mg g^{-1}) > cotton (0.42 mg g^{-1}) > nylon (0.32 mg g^{-1}). The pseudo-second-order kinetic model described the two odor adsorption onto all three fiber types well. Initial adsorption of acetic acid onto wool, cotton, and nylon fiber was mainly controlled by the intraparticle diffusion process, while this is not the case for ammonia adsorption onto the three types of fiber materials. The best odor adsorption and retention

performance of wool fiber is attributed to its large surface area and chemical adsorption mechanism. Cotton fiber had a stronger adsorption towards ammonia than towards acetic acid because of the interaction between hydroxyl groups (–OH) and ammonia *via* hydrogen bonding. Nylon fiber lacked active sites for ammonia adsorption, but it showed remarkable acetic acid adsorption performance due to its predominant basic surface character and the formation of strong hydrogen bonding. This work helps with fiber selection for interior textiles and active sportswear to improve odor management.

Author contributions

Wenli Bai: Investigation, formal analysis, writing – original draft. Hao Yu: data collection. Longlong Liu: data collection. Esfandiar Pakdel: writing – review and editing. Bin Tang: methodology. Hongli Su: resources. Christopher Hurren: writing – review and editing. Lei Liu: investigation. Jinfeng Wang: conceptualization, supervision, writing – review and editing. Xungai Wang: conceptualization, writing – review and editing.

Conflicts of interest

There are no conflicts to declare.

Acknowledgements

We wish to acknowledge support from Deakin University for the PhD scholarship awarded to the first author. Support from the Research Institute for Sports Science and Technology (P0043811) at the Hong Kong Polytechnic University is also acknowledged.

References

1 W. W. Nazaroff and C. J. Weschler, *Indoor Air*, 2020, **30**, 559–644.
2 J. E. Cometto-Muñiz and M. H. Abraham, *Exp. Brain Res.*, 2010, **207**, 75–84.
3 G. D. Nielsen, P. Wolkoff and Y. Alarie, *Regul. Toxicol. Pharmacol.*, 2007, **48**, 6–18.
4 M. A. Smeets, P. J. Bulsing, S. Van Rooden, R. Steinmann, J. A. de Ru, N. W. Ogink, C. van Thriel and P. H. Dalton, *Chem. Senses*, 2007, **32**, 11–20.
5 N. Aldag, J. Gunschera and T. Salthammer, *Cellulose*, 2017, **24**, 4509–4518.
6 E. Höllbacher, T. Ters, C. Rieder-Gradinger and E. Srebotnik, *Eur. J. Wood Wood Prod.*, 2016, **74**, 693–701.
7 S. R. Haines, R. I. Adams, B. E. Boor, T. A. Bruton, J. Downey, A. R. Ferro, E. Gall, B. J. Green, B. Hegarty and E. Horner, *Build Environ.*, 2020, **170**, 106589.
8 A. Saini, J. Okeme, J. Mark Parnis, R. McQueen and M. Diamond, *Indoor air*, 2017, **27**, 631–641.
9 R. H. McQueen, R. M. Laing, C. M. Delahunty*, H. J. Brooks and B. E. Niven, *J. Text. Inst.*, 2008, **99**, 515–523.
10 R. H. McQueen and S. Vaezafshar, *Text. Res. J.*, 2020, **90**, 1157–1173.
11 T. M. Richter, P. J. Bremer, P. Silcock and R. M. Laing, *Text. Res. J.*, 2018, **88**, 2559–2567.
12 R. B. Jørgensen, O. Bjørseth and B. Malvik, *Indoor Air*, 1999, **9**, 2–9.
13 B. Tang, X. Lu, J. Wang, H. Yu, Y. Zhu, S. E. Atkinson and X. Wang, *J. Text. Inst.*, 2021, **112**, 1390–1402.
14 J. Wang, B. Tang, W. Bai, X. Lu and X. Wang, *Adv. Colloid Interface Sci.*, 2020, **283**, 102243.
15 J. Wang, X. Lu, J. Wang and X. Wang, *Text. Res. J.*, 2019, **89**, 2729–2738.
16 A. Elkilani, C. Baker, Q. Al-Shammari and W. Bouhamra, *Environ. Int.*, 2003, **29**, 575–585.
17 E. Pakdel, J. Fang, L. Sun and X. Wang, in *Smart Textiles: Wearable Nanotechnology*, ed. N. D. Yilmaz, Wiley, Hoboken, 2018, Nanocoatings for smart textiles, pp. 247–300.
18 N. Kuwabara, N. Obata and T. Okamoto, *J. Jpn. Soc. Agric. Mach.*, 1999, **61**, 149–156.
19 H. Yu, C. Hurren, X. Liu and X. Wang, *Text. Res. J.*, 2021, **92**, 3060–3070.
20 S. Mohammadi-Jam and K. Waters, *Adv. Colloid Interface Sci.*, 2014, **212**, 21–44.
21 A. Legras, A. Kondor, M. Alcock, M. Heitzmann and R. Truss, *Cellulose*, 2017, **24**, 4691–4700.
22 A. Legras, A. Kondor, M. Heitzmann and R. Truss, *J. Chromatogr. A*, 2015, **1425**, 273–279.
23 J. A. Gamelas, *Cellulose*, 2013, **20**, 2675–2693.
24 W. Tang, J. Wang, W. Bai, R. Rajkhowa, D. Li, B. Tang, X. Wang and W. Xu, *Powder Technol.*, 2022, **400**, 117261.
25 B. Wei, Q. Chen, G. Chen, R. Tang and J. Zhang, *J. Chem.*, 2013, 546839.
26 N. Lazaridis and D. Asouhidou, *Water Res.*, 2003, **37**, 2875–2882.
27 M. M. Nassar, Y. H. Magdy, A. E. H. Daifullah and H. Kelany, *Adsorpt. Sci. Technol.*, 2008, **26**, 157–167.
28 F. Raji and M. Pakizeh, *Appl. Surf. Sci.*, 2014, **301**, 568–575.
29 J. Wang and X. Guo, *J. Hazard. Mater.*, 2020, **390**, 122156.
30 H. Ma, S. Pu, Y. Hou, R. Zhu, A. Zinchenko and W. Chu, *Chem. Eng. J.*, 2018, **345**, 556–565.
31 Q. Hu, Q. Wang, C. Feng, Z. Zhang, Z. Lei and K. Shimizu, *J. Mol. Liq.*, 2018, **254**, 20–25.
32 X. Guo and J. Wang, *J. Mol. Liq.*, 2019, **288**, 111100.
33 V. Vimonses, S. Lei, B. Jin, C. W. Chow and C. Saint, *Chem. Eng. J.*, 2009, **148**, 354–364.
34 Y. Liu, *Colloids Surf., A*, 2008, **320**, 275–278.
35 Y. Shen and N. Zhang, *Bioresour. Technol.*, 2019, **282**, 294–300.
36 M. Frisch, G. Trucks, H. Schlegel, G. Scuseria, M. Robb, J. Cheeseman, G. Scalmani, V. Barone, G. Petersson and H. Nakatsuji, *Gaussian 16 (Revision A)*, Gaussian Inc., Pittsburgh, PA, 2016.
37 S. Grimme, J. Antony, S. Ehrlich and H. Krieg, *J. Chem. Phys.*, 2010, **132**, 154104.
38 K. Raghavachari, *Theor. Chem. Acc.*, 2000, **103**, 361–363.

39 A. McLean and G. Chandler, *J. Chem. Phys.*, 1980, **72**, 5639–5648.
40 F. Weigend and R. Ahlrichs, *Phys. Chem. Chem. Phys.*, 2005, **7**, 3297–3305.
41 W. Bai, M. Qian, Q. Li, S. Atkinson, B. Tang, Y. Zhu and J. Wang, *J. Environ. Chem. Eng.*, 2021, **9**, 105793.
42 A. Kondor, C. Quellet and A. Dallos, *Surf. Interface Anal.*, 2015, **47**, 1040–1050.
43 L. Zhu, D. Shen and K. H. Luo, *J. Hazard. Mater.*, 2020, **389**, 122102.
44 Y. Sun, B. Li, Y. Zhang, H. Dou, W. Fan and S. Wang, *Text. Res. J.*, 2023, **93**, 468–485.
45 M. Wei, F. Marrakchi, C. Yuan, X. Cheng, D. Jiang, F. F. Zafar, Y. Fu and S. Wang, *J. Hazard. Mater.*, 2022, **425**, 127887.
46 W. Tang, B. Tang, W. Bai, E. Pakdel, J. Wang and X. Wang, *J. Cleaner Prod.*, 2022, **366**, 132805.
47 Y. Hu, V. D. Thalangamaarachchige, S. Acharya and N. Abidi, *Cellulose*, 2018, **25**, 4389–4405.
48 L. Reyerson and L. B. Peterson, *J. Phys. Chem.*, 1956, **60**, 1172–1176.